UCRL-94097
PREPRINT

UCRL--94097

DE86 012340

WOLTER X-RAY MICROSCOPE CALIBRATION

Michel Gerassimenko

This paper was prepared for submittal to the Society for Photo-optical Instrumentation Engineers (SPIE) 30th Annual International Technical Symposium on Optical and Optoelectronic Applied Sciences and Engineering, San Diego, California, August 17–22, 1986

June 1986

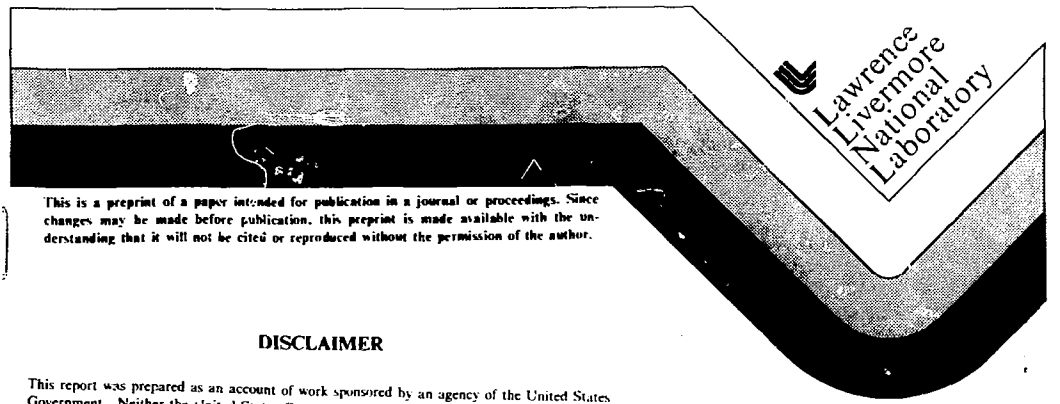

DISCLAIMER

Wolter x-ray microscope calibration

Michel Gerassimenko

University of California, Lawrence Livermore National Laboratory
Mail Stop 43, P.O. Box 808, Livermore, California 94550

Abstract

A 22 × Wolter microscope was calibrated after several months of operation in the Lawrence Livermore National Laboratory (LLNL) Inertial Confinement Fusion program. Placing a point x-ray source at the microscope focus, I recorded the image plane spectrum, as well as the direct spectrum, and from the ratio of these two spectra derived an accurate estimate of the microscope solid angle in the 1–4 keV range. The solid angle was also calculated using the microscope geometry and composition. Comparison of this calculated value with the solid angle that was actually measured suggests contamination of the microscope surface.

Introduction

Axisymmetric hyperboloid-ellipsoid x-ray microscopes have been used in laser fusion programs to provide high spatial resolution in the micron range with a relatively large solid angle.[1,2] Aside from alignment issues, characterization of such a microscope entails (at the very least) spatial resolution and effective solid angle determination. A simple method for determining the effective microscope solid angle is here applied to the 22 × Wolter microscope that has been used in the LLNL Inertial Confinement Fusion program.

Measurement principle

In principle, the microscope solid angle may be related to a simple ratio of incident to focal plane flux. The relation is derived as follows. Consider a source spectrum S(E) extending beyond the high-energy cutoff in the microscope response. The transmission of all filters used in the experimental setup is given by $\eta(E)$, the microscope solid angle by Ω, its reflectivity by R(E), and the detector response by $\epsilon(E)$. The incident flux measured at energy E is then given by

$$D(E) = \int S(x)\eta(x)\epsilon(E - x)\, dx \tag{1}$$

provided that the detector response is normalized. The spatial integral of the flux at the microscope's focal plane is

$$F(E) = \int S(x)\eta(x)\Omega_{eff}(x)\epsilon(E - x)\, dx \tag{2}$$

where $\Omega_{eff}(x) = \Omega \cdot R(E)$ is the effective microscope solid angle.

One of two conditions must be met if Ω_{eff} is to be related to a simple ratio of fluxes. First, if Ω_{eff} in Eq. (2) varies little over the range where ϵ is significant (i.e., over the energy range of the detector resolution), it can be brought outside the integral to give

$$\Omega_{eff}(E) \simeq \frac{F(E)}{D(E)} . \tag{3}$$

Alternatively, if Ω_{eff} varies substantially over the range where ϵ is significant, and $S \cdot \eta$ varies slowly over the same region, then

$$\frac{F(E)}{D(E)} \simeq \int \Omega_{eff}(x)\epsilon(E - x)\, dx . \tag{4}$$

It turns out that one or the other of these two conditions is in fact met for measurements made in the 1–4 keV range discussed below. Thus, the ratio F(E)/D(E) approximates the average value of $\Omega_{eff}(E)$ over the energy range of the detector resolution.

Measurement technique

Figure 1 shows the physical setup for the solid-angle measurements. During normal operation a pre-filter is placed in front of the electroless nickel microscope to protect it from target debris. In order to match these operational conditions, a pre-filter is installed for the calibration as well. The source is positioned 291.5 mm in front of the microscope.

The x-ray source illuminating the microscope must be sufficiently small to fit within the instrument's field of view. It must also produce x-rays over the energy range of interest. The low-energy limit is set at about 1 keV by the pre-filter transmission, while the high-energy limit is about 4 keV. This is the level at which reflectivity becomes negligible for the electroless nickel.

The point source described in Price, Boyle, and Glaros meets these requirements.[3] It consists of a single-turn filament and a tungsten needle that is operated at several kV. With a focal plane image that is roughly 400 μ in diameter, the source size is deduced to be about 20 μ. A sketch of the x-ray source is shown in Figure 2.

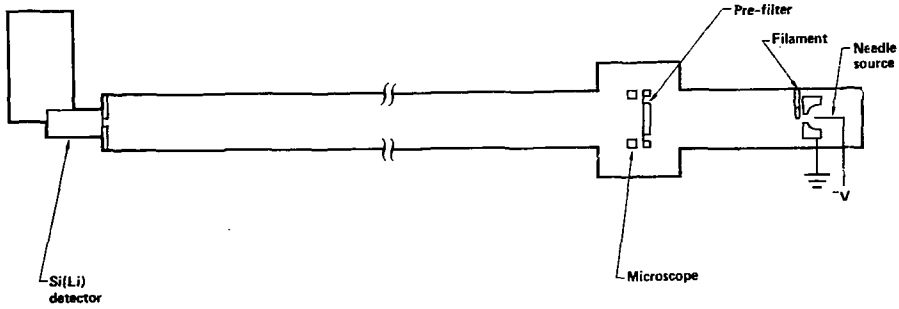

Figure 1. The experimental setup for solid-angle measurements.

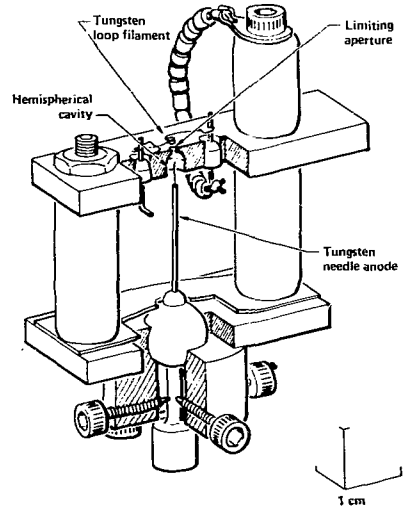

Figure 2. X-ray point source assembly (after Price, Boyle, and Glaros[3]). Since the focal plane image measured 400 μ in diameter, the source size is deduced to be roughly 20 μ.

A Si(Li) detector is used to measure the x-ray source spectrum D(E). This spectrum (shown in Figure 3) is relatively flat in the 1–4 keV range except for the tungsten M line at 1.77 keV. The full width half maximum detector resolution at the line energy is 150 eV. Fortunately, for two reflections at the 1 deg angle used in the microscope, the calculated reflectivity of electroless nickel varies slowly between 1.5 and 2 keV (Figure 4). *Reflectivity is calculated using the composition of the microscope material (87% nickel by weight with the balance phosphorus at an overall density* of 7.9 g/cm^3) and tabulated constants.[4]

The focal plane spectrum F(E) is displayed in Figure 5, and some experimental parameters are listed in Table 1. Energy calibration of the multichannel analyzer is deduced from the measured position of the tungsten M line, and the position of the Fe Kα line was obtained during a calibration run.

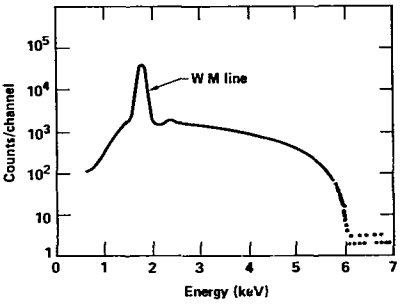

Figure 3. Source spectrum D(E) incident upon the microscope. Parameters of the Si(Li) detector system are listed in Table 1, *under the heading "Instrument Settings."*

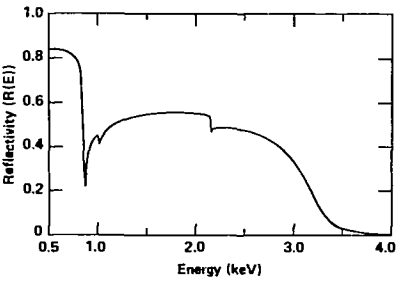

Figure 4. Reflectivity of electroless nickel for two reflections at 1 deg, calculated using the data supplied in Reference 4.

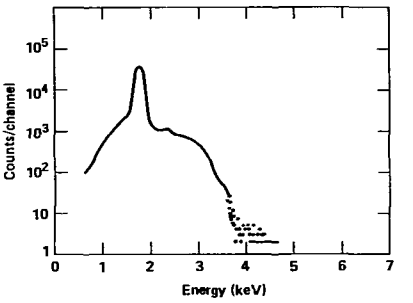

Figure 5. Focal plane spectrum *F(E)*. Detector system parameters are listed in Table 1 under the heading, "Instrument Settings."

Table 1. Calibration Parameters

Source		Instrument Settings	
Needle: 6 deg cone angle Filament: 1 turn, 20 mils ID Needle tip to base front: 1 mm Spot size in microscope image plane: 0.4-mm diameter		Kevex Si(Li) Detector bias: 500 V Preamp: gain X4, fine gain 0.6 shaping 6 SCA: 0.25–10 V ND575: Conv. gain 8K	
	Direct Spectrum		Focal Plane Spectrum
Source settings:	6 kV, 230 nA		6 kV, 150 nA
SCA count rate:	470 cts/s		530 cts/s
Live time:	6000 s/unit (5 units acquired)		6000 s/unit (5 units acquired)
Aperture diameter:	1.27 mm		1.27 mm
Source tip to detector aperture:	163.2 mm		

Results

The ratio F(E)/D(E) as it appears in Figure 6 is a good estimate of $\Omega_{eff}(E)$. The fact that fluctuations in the data are due to count rate statistics is evident by their smaller amplitude in the 1.6- to 1.9-keV range where the W-line x-rays are binned. The continuity of the curve over the W-line region is an indication of the stability in the experimental conditions achieved during the measurements.

It is interesting to compare the measured effective solid angle (Figure 6) with the calculated values [$\Omega_{eff} = \Omega \cdot R(x)$] displayed in Figure 4. Agreement between the measured and calculated values is improved slightly by convolving the calculated solid angle with the detector resolution. The resolution is taken to be Gaussian with the standard deviation being a constant fraction of the energy. Its value was fitted from the W-line data in the direct spectrum shown in Figure 3.

The convolved calculated solid angle is shown in Figure 7, and the ratio of measured to calculated solid angles is given in Figure 8. A small number of pulses pile up at twice the tungsten M line energy, affecting the ratio above 3.4 keV. A trend is evident in the data, one that reveals the ratio as a monotonically decreasing function of energy.

The near unity ratio at 1 keV is an indication of the smoothness of the microscope surface, since roughness produces large angle scattering, and this scattering removes energy from the integrated spectrum at the focal plane. As one moves to higher energies the ratio steadily decreases, dropping below 0.2 at 3.4 keV. This behavior suggests that the microscope has been contaminated before calibration, during its months of use on the Shiva laser at LLNL. An oil film or any other organic residue admixed to the microscope surface could produce the type of energy dependence seen in the ratio. Another possible reason for the lowered ratio would be small-scale surface roughness, but comparison of the data reported here with cruder measurements performed prior to microscope installation favor the contamination hypothesis.

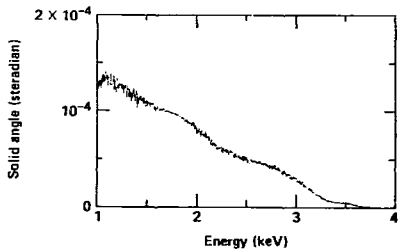

Figure 6. The ratio of F(E)/D(E) provides a good estimate of the effective microscope solid angle.

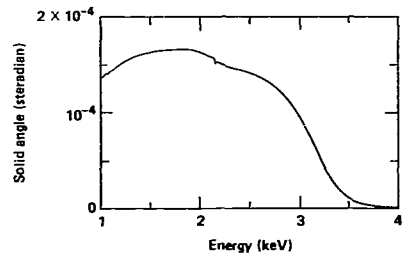

Figure 7. Calculated effective microscope solid angle using the microscope geometry and the electroless nickel reflectivity. The solid angle has been convolved with the detector resolution to give better agreement with the measured values displayed in Figure 6.

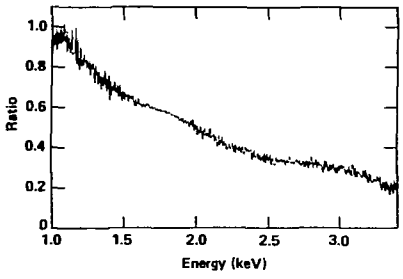

Figure 8. Ratio of measured to calculated effective microscope solid angles.

Conclusion

The fairly straightforward measurements of spectra incident upon the microscope and at its focal plane have yielded a reasonable estimate of the microscope solid angle over its useful energy range. The measured solid angle is close to that calculated near 1 keV, and decreases to only two tenths of the value calculated at 3.4 keV. This energy dependence was most likely caused by contamination of the microscope surface.

Acknowledgments

I am grateful to Robert H. Price, who both designed and operated the microscope, and who pioneered the calibration scheme described in this work. William M. Cook was a full participant in all phases of the characterization effort. This work was performed under the auspices of the U.S. Department of Energy by the Lawrence Livermore National Laboratory under contract No. W-7405-Eng-48.

References

1. Price, R. H., "X-Ray Microscopy Using Grazing Incidence Reflection Optics," AIP Conf. Proc., Vol. 75, p. 189. 1981.
2. Obenschain, S. P., R. R. Whitlock, E. A. McLean, B. H. Ripin, R. H. Price, D. W. Phillion, E. M. Campbell, M. D. Rosen, and J. M. Auerbach, "Uniform Ablative Acceleration of Targets by Laser Irradiation at 10^{15} W/cm^2," Phys. Rev. Lett., Vol. 50, No. 44. 1983.
3. Price, R. H., M. J. Boyle, and S. S. Glaros, Point X-Ray Source, Lawrence Livermore National Laboratory, Livermore, CA, UCRL-81643. 1978.
4. Henke, B. L., P. Lee, T. J. Tanaka, R. L. Shimabukuro, and B. K. Fujikawa, "Low-Energy X-Ray Interaction Coefficients," in Atomic Data and Nuclear Data Tables, Vol. 27, No. 1. 1982.